Cu-Zn-Sn-S Thin Films from Electrodeposited Metallic Precursor Layers

Raghu N. Bhattacharya* and J.Y. Kim

National Renewable Energy Laboratory, 1617 Cole Boulevard, Golden, Colorado 80401, USA

Abstract: Cyclic voltammogram of ionic liquid and metallic-salts in ionic liquids were recorded. Cu/Sn/Zn stacked layers were electrodeposited and subsequently sulfurized in a tube furnace in elemental sulfur at 550ºC. Thin films were characterized by X-ray diffraction, ICP-MS, and SEM. The device was characterized by I-V, QE and Mott-Schottky (capacitance-voltage) plot.

Keywords: Cu-Zn-Sn-S, thin films, electroplated, cyclic voltammogram.

1. INTRODUCTION

Photovoltaic (PV) solar electric technology will be a significant contributor to world energy supplies when reliable, efficient PV power products are manufactured in large volumes at low cost. A promising pathway to reducing PV cost is the use of thin-film technologies in which thin layers of photoactive materials are deposited inexpensively on large-area substrates. The primary chalcogenide semiconductor absorber materials currently used for thin-film PV device applications are $Cu(In,Ga)Se_2$ and CdTe. Despite the promise of these technologies, the toxicity of Cd and supply limitations for In and Te are projected to limit the production capacity of these existing chalcogen-based technologies to <100 GWp per year. This represents a small fraction of the world's growing energy needs, which are expected to double to 27 TW by 2050. Therefore, a lot of efforts have been made recently to explore new absorber materials with nontoxic and earth-abundant elements. One prominent example of the alternative solar cell materials is Cu_2ZnSnS_4 (CZTS). CZTS has a direct band gap of 1.45 − 1.6 eV and an optical absorption coefficient of around 10^5 cm^{-1} [1, 2]. Recently several groups reported a CZTS thin-films fabrication method using a variety of fabrication methods, namely sputtering [2-5], physical vapor deposition [6-11], a solution-particle approach [12-14], photochemical deposition [15], the sol-gel method [16], screen-printing [17], and electroplating [18-26]. The best conversion efficiency of the CZTS solar cell is reported to be 10% [12-14]. The electroplated CZTS solar cell also demonstrated a respectable 7.3%-efficient device [26].

Electroplating is a potentially suitable preparation method to obtain low-cost precursor films. The electrodeposition process could provide: (a) high-quality film with very low capital investment; (b) a low-cost, high-rate process; (c) use of very low-cost starting materials (e.g., low-purity salts or solvents), based on automatic purification of the deposited materials during plating; (d) a large-area, continuous, multi-component, low-temperature deposition method; (e) deposition of films on a variety of shapes and forms (wires, tapes, coils, and cylinders); (f) controlled deposition rates and effective material use (as high as 98%); and (g) minimum waste generation (i.e., the solution can be recycled).

Most of the electrodeposited CZTS precursor films reported are prepared from aqueous electrolyte solutions. The electrodeposition of an element (e. g., Sn) that has a standard reduction potential more negative than the water reduction potential becomes very difficult due to the competition between electroplating of the desired element and water electrolysis. To avoid the water reduction issue, electrodeposition needs to be done using non-aqueous solvents with a large electrochemical window, like ionic liquids (ILs).

In this study, CZTS thin films have been prepared by electrodeposition of multilayered Cu-Sn-Zn metal films on Mo/glass substrates from ionic liquid solvents. The electro-deposited thin-film precursor films are subsequently sulfur-ized in a tube furnace in an elemental sulfur environment.

2. EXPERIMENTAL PROCEDURE

In general, electrodeposition of Cu-Sn-Zn was performed sequentially from a Cu-plating solution, Sn-plating solution, and Zn-plating solution, respectively. First, a Cu layer was electrodeposited on a Mo/glass substrate from a Cu-plating solution, the second Sn layer was electrodeposited from a Sn-plating solution, and the third Zn layer was electro-deposited from a Zn-plating solution. The solution concentrations of each deposition solutions were 0.1 M. Fisher Scientific (FB300) and VWR (300V) power supplies were used to electrodeposit Cu-Sn-Zn thin films. All films were electrodeposited by applying constant current. Cu was plated at −4.2 mA/cm^2 for 3 minutes, Sn was plated at −2.0 mA/cm^2 for 10 minutes and Zn was plated at −1.7 mA/cm^2 for 8 minutes. The desired film composition was obtained by adjusting the film thickness of Cu, Sn and Zn. The films were electrodeposited in a vertical cell in which the electrodes (both working and counter) were suspended vertically from the top of the cell. Precursor films were prepared by employing a two-electrode cell in which the counter electrode was Pt gauze and the working electrode (substrate) was glass/Mo. The Mo film was about 1 μm thick and was deposited by direct current (dc) sputtering. All

*Address correspondence to this author at the National Renewable Energy Laboratory, 1617 Cole Boulevard, Golden, Colorado 80401, USA; Tel: 303-384-6477; Fax: 303-384-6432; E-mail: raghu.bhattacharya@nrel.gov

1876-5319/12

chemicals were of Analar- or Puratronic-grade purity and were used as received. The film compositions were analyzed using Agilent Technolgies 7700 Series ICP-MS system. X-ray diffraction (XRD) was performed by a Scintag X-ray machine using a Copper K_α radiation at $\lambda = 0.5456$ Å. PV devices were completed by chemical-bath deposition of about 50 nm CdS, followed by radio frequency (RF) sputtering of 50 nm of intrinsic ZnO and 350 nm of Al_2O_3-doped conducting ZnO. Bilayer Ni/Al top contacts were deposited in an e-beam system.

3. RESULTS AND DISCUSSION

Cyclic voltammograms (CVs) were obtained at 53°C with a scan rate of 50 mV/s using a potentiostat (Princeton, VCM-4) with a 3-electrode system composed of Pt-working, Pt-counter, and Pt-quasi reference electrodes. The measurements were performed after the open circuit voltage of the electrochemical cell was stabilized (usually 1 hour). Fig. (**1a**) shows a CV curve of the choline chloride-based ionic liquid used in this study. The water reduction peak at V ≈ 0.9 V *vs* Pt, indicates a trace amount of water present in the

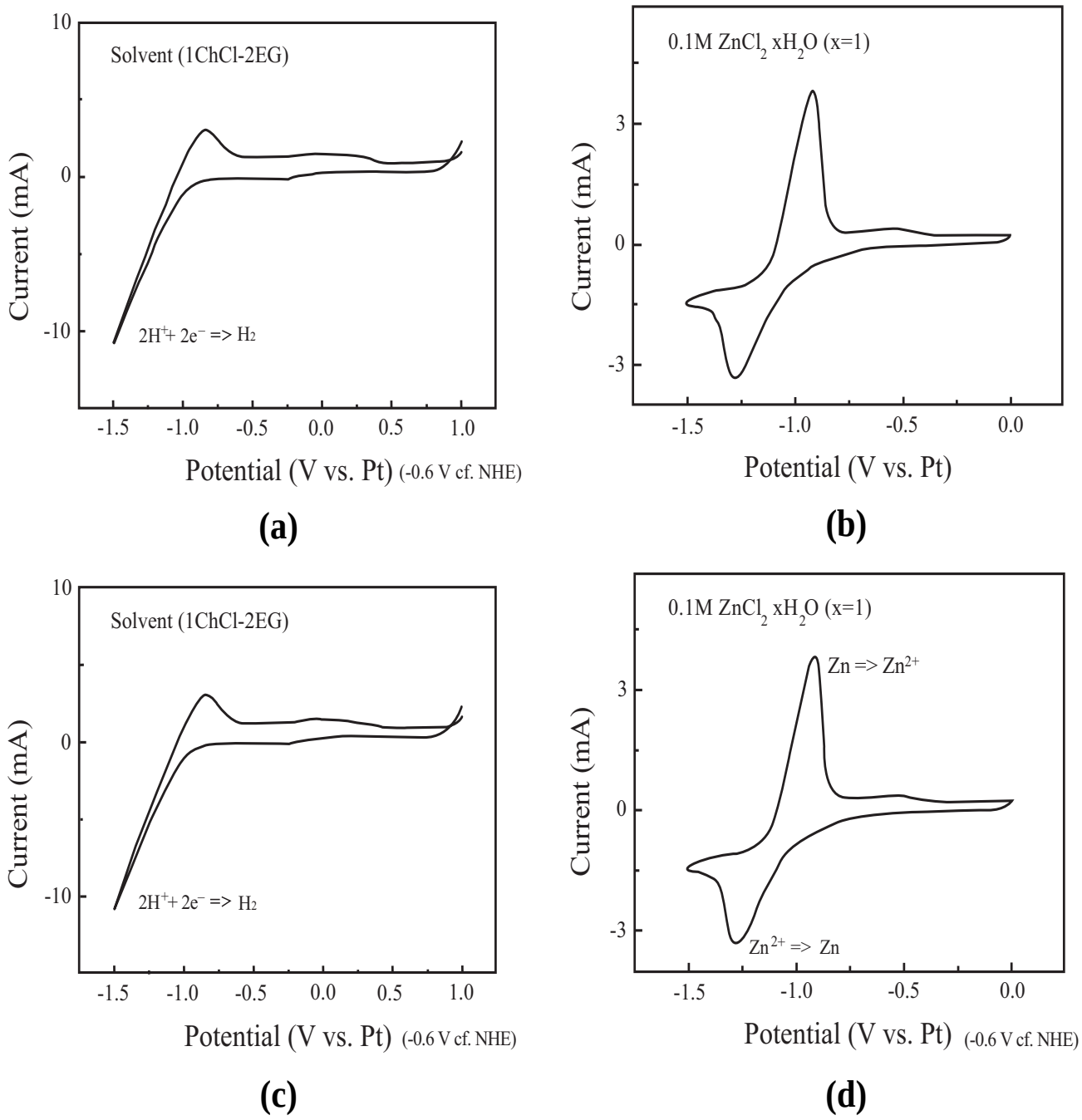

Fig. (1). (**a**) CV of the ionic liquid; (**b**) CV of 0.1 M $ZnCl_2$ in ionic liquid; (**c**) CV of 0.1 M $SnCl_2$ in ionic liquid; (**d**) CV of 0.1 M $CuCl_2$. All CVs were performed at 53ºC.

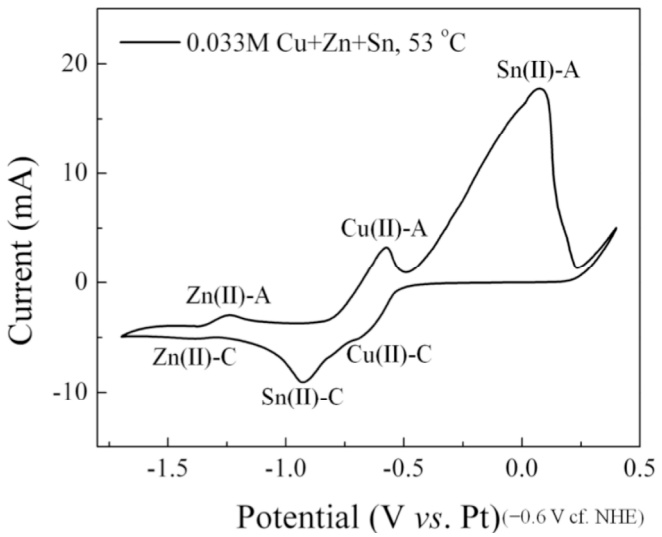

Fig. (2). CV of 0.033 M $CuCl_2$, $ZnCl_2$, and $SnCl_2$ in ionic liquid at 53ºC.

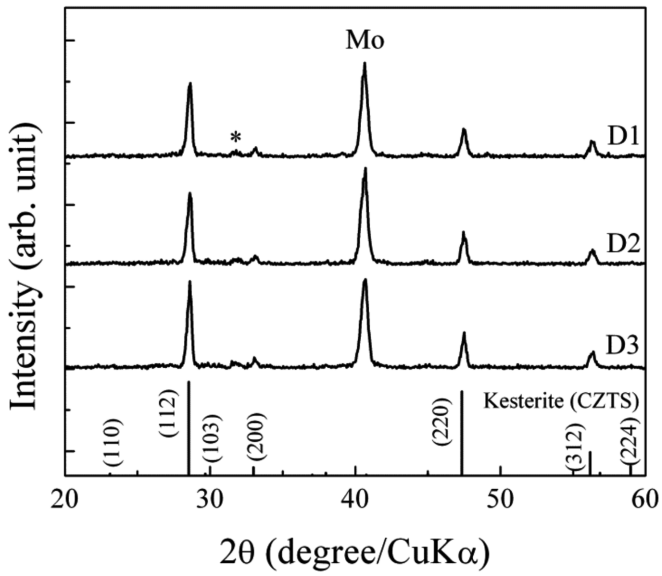

Fig. (3). X-ray diffractions of annealed Cu-Zn-Sn-S thin films (D1, D2, and D3 samples were prepared under similar condition to check the reproducibility).

ionic liquid solvent. Fig. (**1b**) shows the CV curve of 0.1 M $ZnCl_2{\cdot}H_20$ in choline chloride-based ionic liquid solution. The CV curve shows the Zn-reduction ($Zn^{2+} + 2e^- \Rightarrow Zn$) and Zn-oxidation ($Zn \Rightarrow Zn^{2+} + 2e^-$) peaks at −1.28 V and −0.92 V (*vs* Pt), respectively. The standard reduction potential of Zn(II) ($Zn^{2+} + 2e^- \Rightarrow Zn$) is −0.76 V *vs* standard hydrogen electrode (SHE) in 1 M aqueous solution at 25°C [27]. Fig. (**1c**) shows the CV curve of 0.1 M $SnCl_2{\cdot}H_20$ in choline chloride-based ionic liquid solution. The CV curve shows reduction ($Sn^{2+} + 2e^- \Rightarrow Sn$) and oxidation ($Sn \Rightarrow Sn^{2+} + 2e^-$) peaks of Sn at −0.89 V and 0.06 V (*vs* Pt), respectively. The standard reduction potential of Sn(II) ($Sn^{2+} + 2e^- \Rightarrow Sn$) is −0.14 V *vs* SHE in 1 M aqueous solution at 25°C [27]. A larger reduction potential shift is observed for Sn compared with Zn, when a Pt-quasi reference electrode is used in ionic liquid solvent. Fig. (**1d**) shows the CV curve of 0.1 M $CuCl_2$ in choline chloride-based ionic liquid solution. The CV curve shows two reduction peaks at −0.25 V and −0.57 V, respectively. The standard reduction potential for Cu ions is 0.52 V and 0.34 V *vs* SHE in 1 M aqueous solution at 25°C [27]. Fig. (**2**) shows the CV curve of 0.03 M $CuCl_2$, 0.03 M $ZnCl_2$, and 0.03 M $SnCl_2$ in choline chloride-based ionic solution. The CV curve indicates that all metal ions could be co-deposited from the ionic liquid solvents. The significant reduction potential shifts of Zn, Sn, and Cu are attributed to Pt-quasi reference electrode and over-potential imposed by ionic liquid solvent. These reduction potential values are only useful to preset the deposition potential/current from the ionic liquid solution.

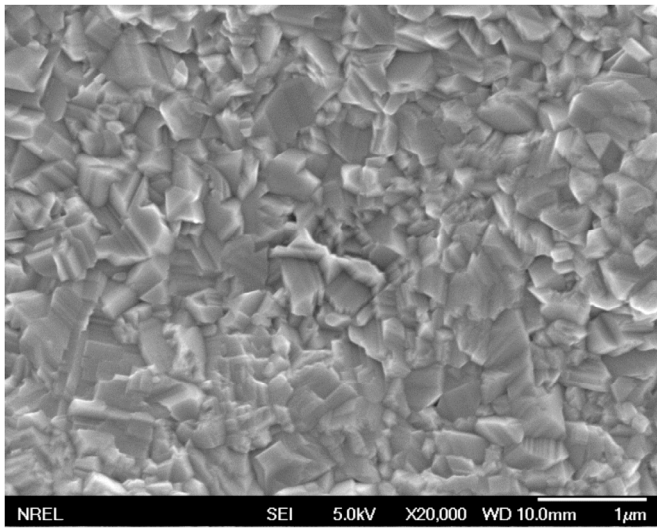

(a)

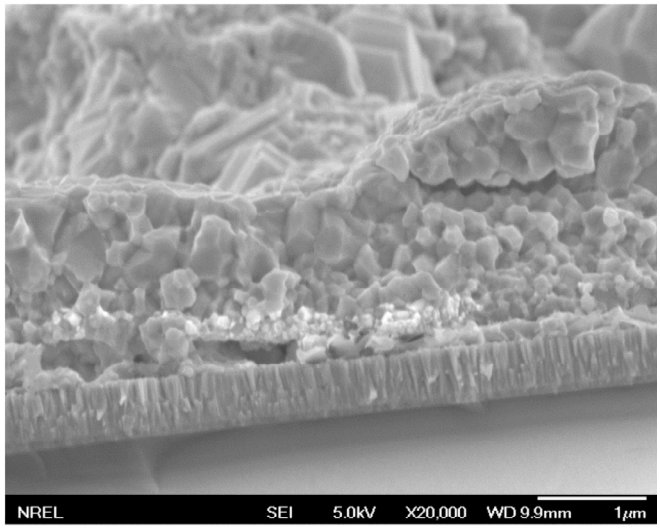

(b)

Fig. (4). (**a**) SEM surface morphology; (**b**) SEM cross-section of annealed CZTS thin films.

Fig. (**3**) shows the X-ray diffraction (XRD) patterns of three annealed CZTS thin films (D1, D2 and D3). The precursor electrodeposited Cu/Sn/Zn stacked layers were annealed in a tube furnace at 550ºC in elemental S atmosphere for 60 minutes. All samples were prepared at

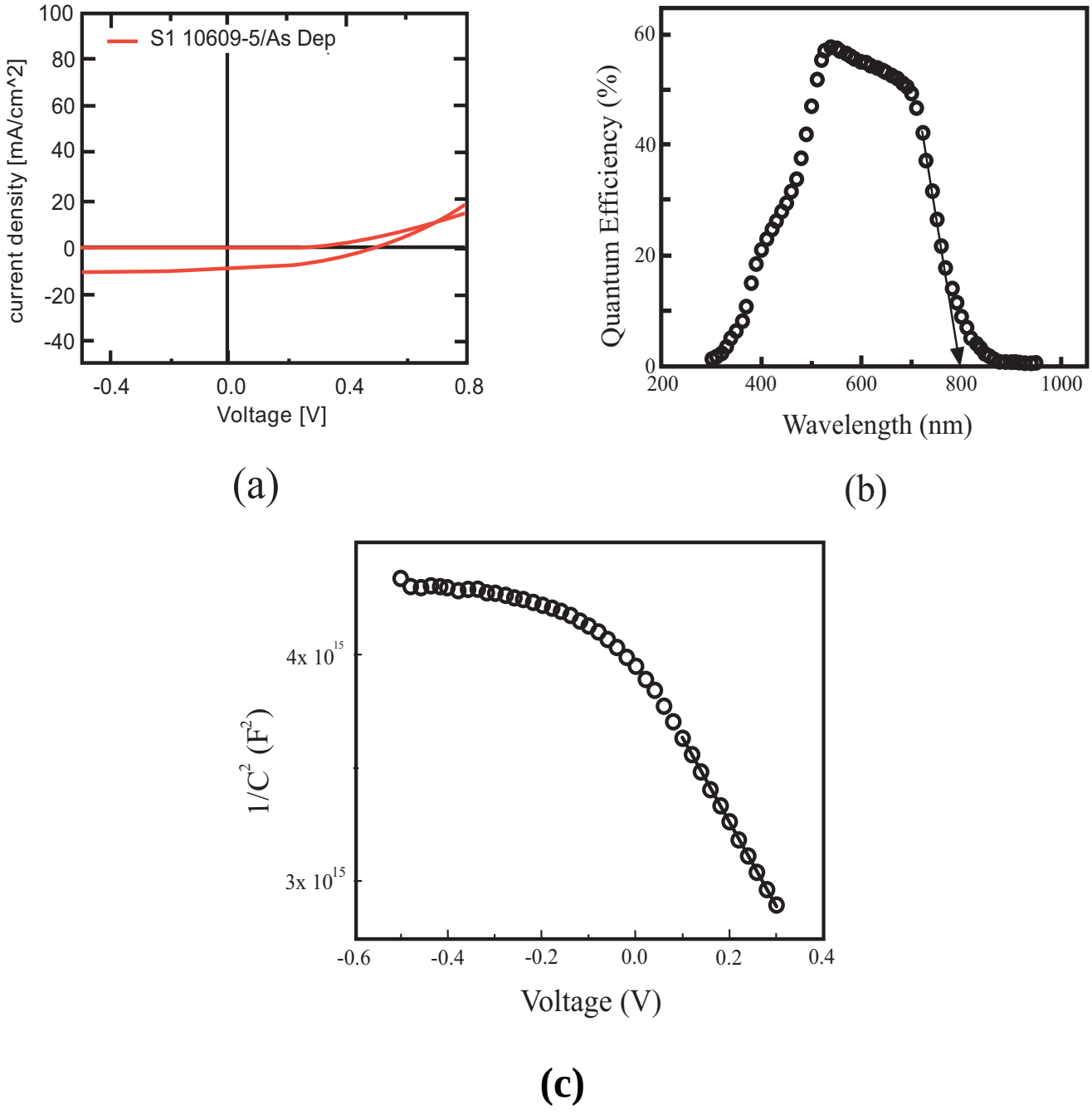

Fig. (5). (**a**) Current-voltage characteristics: V_{oc} = 0.51 V, J_{sc} = 9 mA/cm^2, fill factor = 37%, and efficiency = 1.7%; (**b**) QE characteristics of the device; (**c**) Mott-Schottky plot of the CZTS device.

same condition (Cu: −4.2 mA/cm^2, 3 min, Sn: −2.0 mA/cm^2, 10 min, Zn: −1.7 mA/cm^2, 8 min) to check the reproducibility of the deposition conditions. The precursor film compositions of the films, as analyzed by ICP-MS, were Cu:47-49 at%; Zn:27-25 at%, and Sn:26-24 at%. As shown in Fig. (**3**), the XRD patterns are almost identical for all three samples representing Kesterite CZTS structure [joint committee on powder diffraction standards (JCPDS) # 26-0575]. The small XRD peak at 32^o is attributed to the $Cu_{1.95}S$ or SnS_2 impurity phase [24]. The surface morphology and cross-sectional view (SEM) of a representative film annealed at 550ºC for 60 minutes is shown in Fig. (**4a**, **b**). The SEM as shown in Fig. (**4a**, **b**), indicate that films are crack-free and have a compact dense morphology. The cross-sectional

view (Fig. **4b**) of the film shows the film thickness is about 1.3 μm and it has a very rough surface morphology. The grain size determined from the top-view and cross-sectional images ranged from about 100 to 500 nm, and the grains exhibit sharp facets. This result indicates that we need to further optimize the deposition and processing conditions to obtain smooth and uniform films. Solar cell devices were fabricated from these absorber materials. The device efficiency (Fig. **5a**) that resulted from the processed electrodeposited precursor film was only 1.7% with a respectable V_{oc} (0.51 V), but very poor J_{sc} (9 mA/cm^2) and poor fill factor (37.5). Very poor fill factor and J_{sc} are probably due to poor film morphology and presence of secondary phases. In this study, the samples were not treated with KCN, so some conducting phases like Cu_xS (as shown by XRD) were present in the films. Chemical etching with KCN solution, which is known to remove Cu_xS phase effectively, will be incorporated in the future experiments. In addition, the partial pressure of vaporized S can be better controlled by using H_2S gas for forming S atmosphere rather than using elemental S as the source. Fig. (**5b**) displays the external quantum efficiency (EQE) spectrum of the device. The maximum quantum efficiency is as high as 60% at 550 nm and the J_{sc} calculated by integrating the spectrum (~10 mA/cm^2) is in good agreement with the measured J_{sc} (9 mA/cm^2). This EQE spectrum also reveals that the optical band gap of the CZTS thin film is ~1.55 eV (800 nm). Fig. (**5c**) shows the Mott-Schottky (capacitance-voltage) plot of the CZTS solar cells. The charge carrier concentration ($p + N_A$) calculated from the slope (linear fit) is ~4×10^{16} cm^{-3}, which is significantly lower than the reported values of 3.81 x 10^{18} cm^{-3} for 0.49%-efficient screen-printed CZTS thin films [17].

4. CONCLUSION

CV measurements were performed to understand the electrochemical behavior of the metal-salts in ionic liquid solutions. Electrodeposited CZTSS absorber layers are fabricated by annealing stacked Cu/Sn/Zn layers in the tube furnace in the presence of elemental sulfur. The absorber material used for the device fabrication has very low carrier concentration and so the device has only 1.7% efficiency. We are expecting to improve the device efficiency by processing the stacked layer in H_2S at high temperature.

ACKNOWLEDGEMENTS

The authors thank Clay DeHart (NCPV, NREL) for device fabrication. This work has been performed by an employee of the Alliance for Sustainable Energy, LLC, under contract number DE-AC36-08GO28308 with the U.S. Department of Energy. The United States Government retains a nonexclusive, paid-up, irrevocable, worldwide license to publish or reproduce the published form of this work, or allow others to do so, for United States Government purposes.

CONFLICT OF INTEREST

The authors declare that they have no competing interests.

REFERENCES

[1] Jimbo K, Kimura R, Kamimura T, *et al*. Cu_2ZnSnS_4-type thin film solar cells using abundant materials. Thin Solid Films 2007; 515: 5997-9.

[2] Ito K, Nakazawa T. Electrical and optical properties of stannite-type quaternary semiconductor thin films. Jpn J Appl Phys 1998; 27: 2094-7.

[3] Chalapathy RBV, Jung GS, Ahn BT. Fabrication of Cu_2ZnSnS_4 films by sulfurization of Cu/ZnSn/Cu precursor layers in sulfur atmosphere for solar cells. Sol Energy Mater Sol Cells 2011; 95: 3216-21.

[4] Tanaka T, Nagatomo T, Kawasaki D, *et al*. Preparation of Cu_2ZnSnS_4 thin films by hybrid sputtering. J Phys Chem Solids 2005; 66: 1978-81.

[5] Seol JS, Lee SY, Lee JC, Nam HD, Kim KH. Electrical and optical properties of Cu_2ZnSnS_4 thin films prepared by rf-magnetron sputtering process. Sol Energy Mater Sol Cells 2003; 75: 155-62.

[6] Oishi K, Saito G, Ebina K, *et al*. Growth of Cu_2ZnSnS_4 thin films on Si (100) substrates by multisource evaporation. Thin Solid Films 2008; 517: 1449-52.

[7] Katagiri H, Sasaguchi N, Hando S, Hoshino S, Ohashi J, Yokota T. Preparation and evaluation of Cu_2ZnSnS_4 thin films by sulfurization of E−B evaporated precursors. Sol Energy Mater Sol Cells 1997; 49: 407-14.

[8] Katagiri H, Saitoh K, Washio T, Shinohara H, Kurumadani T, Miyajima S. Development of thin film solar cell based on Cu_2ZnSnS_4 thin films. Sol Energy Mater Sol Cells 2001; 65: 141-8.

[9] Grenet L, Bernardi S, Kohen D, *et al*. $Cu_2ZnSn(S_{1-x}Se_x)_4$ based solar cell produced by selenization of vacuum deposited precursors. Sol Energy Mater Sol Cells 2012; 101: 11-4.

[10] Wang K, Gunawan O, Todorov T, Shin B, Vhey SJ, Bojarczuk NA. Structural and elemental characterization of high efficiency Cu_2ZnSnS_4 solar cells. Appl Phys Lett 2011; 98: 051912.

[11] Salome PMP, Malaquias J, Fernandes PA, *et al.* Growth and characterization of $Cu_2ZnSn(S,Se)_4$ thin films for solar cells. Sol Energy Mater Sol Cells 2012; 101:147-53.

[12] Mitzi DB, Gunawan O, Todorov TK, Wang K, Guha S. The path towards a high-performance solution-processed kesterite solar cell. Sol Energy Mater Sol Cells 2011; 95: 1421-36.

[13] Todorov TK, Reuter KB, Mitzi DB. High-Efficiency Solar Cell with Earth-Abundant Liquid-Processed Absorber. Adv Mater 2010; 22: E156-9.

[14] Barkhouse DAR, Gunawan O, Gokmen T, Todorov TK, Mitzi DB. Device characteristics of a 10.1% hydrazine-processed $Cu_2ZnSn(Se,S)_4$ solar cell. Prog Photovoltaics Res Appl 2012; 20: 6-11.

[15] Shin B, Zhu Y, Gunawan O, Bojarczuk NA, Chey SJ, Guha S. Thin film solar cell with 8.4% power conversion efficiency using an earth-abundant Cu_2ZnSnS_4 absorber. Prog Photovolt: Res Appl 2011; doi: 10.1002/pip.1174.

[16] Moriya K, Tanaka K, Uchiki H. Characterization of Cu_2ZnSnS_4 thin films prepared by photo-chemical deposition. Jpn J Appl Phys 2005; 44: 715-7.

[17] Zhou ZH, Wang Y, Xu D, Zhang Y. Fabrication of Cu_2ZnSnS_4 screen printed layers for solar cells. Sol Energy Mater Sol Cells 2010; 94: 2042-5.

[18] Tanaka K, Oonuki M, Moritake N, Uchiki H. Cu_2ZnSnS_4 thin film solar cells prepared by non-vacuum processing. Sol Energy Mater Sol Cells 2009; 93: 583-7.

[19] Araki H, Kubo Y, Jimbo K, *et al*. Preparation of Cu_2ZnSnS_4 thin films by sulfurization of co-electroplated Cu-Zn-Sn precursors. Phys Status Solidi C 2009; 61: 1266-8.

[20] Kurihara M, Berg D, Fisher J, Siebentritt S, Dale PJ. Kesterite absorber layer uniformity from electrodeposited pre-cursors. Phys Status Solidi C 2009; 6: 1241-4.

[21] Ennaoui A, Lux-Steiner M, Abou-Ras D, *et al*. Cu_2ZnSnS^4 thin film solar cells from electroplated precursors: Novel low-cost perspective. Thin Solid Films 2009; 517: 2511-4.

[22] Pawar SM, Pawar BS, Moholkar AV, *et al.* Single step electrosynthesis of Cu_2ZnSnS_4 (CZTS) thin films for solar cell application. Electrochimica Acta 2010; 55: 4057-61.

[23] Chan CP, Lam H, Surya C. Preparation of Cu_2ZnSnS_4 films by electrodeposition using ionic liquids. Sol Energy Mater Sol Cells 2010; 94: 207-11.

[24] Schurr R, Holzing A, Jost S, *et al*. The crystallisation of Cu_2ZnSnS_4 thin film solar cell absorbers from co-electroplated Cu–Zn–Sn precursors. Thin Solid Film 2009; 517: 2465-8.

[25] Deligianni H, Ahmed S, Romankiw LT. The Next Frontier: Electrodeposition for Solar Cell Fabrication. Interface 2011; 20: 47-53.

[26] Ahmed S, Reuter KB, Gunawan O, Gao L, Romankiw LT, Deligianni H. A high efficiency electrodeposited Cu_2ZnSnS_4 solar cell .Adv Energy Mater 2012; 2: 253-9.

[27] CRC Handbook of Chemistry and Physics. David R, Ed. 74th ed. Boca Raton: CRC Press 1993-1994.

Received: May 26, 2012 Revised: June 18, 2012 Accepted: June 30, 2012